

Fragmentation of Fractal Random Structures

Eren Metin Elçi,^{1,*} Martin Weigel,^{1,2,†} and Nikolaos G. Fytas^{1,‡}

¹*Applied Mathematics Research Centre, Coventry University, Coventry CV1 5FB, England*

²*Institut für Physik, Johannes Gutenberg-Universität Mainz, Staudinger Weg 7, D-55099 Mainz, Germany*

(Received 7 November 2014; published 20 March 2015)

We analyze the fragmentation behavior of random clusters on the lattice under a process where bonds between neighboring sites are successively broken. Modeling such structures by configurations of a generalized Potts or random-cluster model allows us to discuss a wide range of systems with fractal properties including trees as well as dense clusters. We present exact results for the densities of fragmenting edges and the distribution of fragment sizes for critical clusters in two dimensions. Dynamical fragmentation with a size cutoff leads to broad distributions of fragment sizes. The resulting power laws are shown to encode characteristic fingerprints of the fragmented objects.

DOI: 10.1103/PhysRevLett.114.115701

PACS numbers: 64.60.F-, 05.50.+q, 05.70.Ln

Breakup phenomena are ubiquitous in nature and technology [1]. They span a vast range of time and length scales, including polymer degradation [2] as well as collision induced fragmentation of asteroids [3]. In geology, fragmentation results in the distribution of grain sizes observed in soils; fluids break up into droplets and fluid structures such as eddies undergo fragmentation [4]. On the subatomic scale, excited atomic nuclei break up into fragments [5]. Practical applications, such as mineral processing, ask for optimizations according to technological requirements and efficiency considerations [1]. More generally, a wide range of structures from transport systems to social connections are described by complex networks, whose degree of resilience against fragmentation is a recent subject of intense scrutiny [6,7].

Considerable effort has been invested in defining and analyzing tractable models of fragmentation processes [1,8]. For brittle materials, in particular, spring or beam models as well as finite-element techniques have been used to describe the formation and propagation of cracks in problems of fracture and *instantaneous* fragmentation [8–10], and these models allow one to describe a range of experimental observations [11–14]. In contrast, the fragment-size distribution (FSD) $n(s, t)$ for *continuous* fragmentation such as in milling or the breakup of fluids can be described stochastically by rate equations of the form [1]

$$\frac{\partial n(s, t)}{\partial t} = - \int_0^s n(s, t) c(s, s', t) ds' + 2 \int_s^\infty n(s', t) c(s', s, t) ds', \quad (1)$$

where $c(s, s', t) = a(s, t)b(s, s', t)$, $a(s, t)$ denotes the fragmentation rate of clusters of mass s , and $b(s, s', t)$ is the conditional probability for an s breakup event to result in a fragment of size s' . Here, the first term on the r.h.s. describes

the loss of fragments at size s due to breakup, whereas the second term corresponds to the gain from the breakup of clusters of mass larger than s . In practice, the kernel is normally assumed to be time independent, $c(s, s', t) \equiv c(s, s')$. Additionally, a description through Eq. (1) implies a fragmentation process that is spatially homogeneous and independent of fragment shape—clearly a drastic simplification. Under such assumptions a useful scaling theory of solutions can be formulated [15,16].

Much less progress has been made in terms of results beyond this mean-field approximation. What is the relation between geometrical properties of fragmented objects and the resulting FSDs? This has been studied for loopless structures such as intervals [17–20] and trees [21]. For higher-dimensional shapes the only results to date concern the fragmentation of percolation clusters [22–25]. It was demonstrated numerically there that the fragmentation rate $a(s)$ as well as the conditional breakup probability $b(s, s')$ exhibit power-law scaling.

In the present Letter we discuss fragmentation within a generalization of the percolation model with bond activation probability p , additional cluster weight q , and partition function

$$Z_{\text{RC}} = \sum_{\mathcal{G}' \subseteq \mathcal{G}} p^{b(\mathcal{G}')} (1-p)^{\mathcal{E}-b(\mathcal{G}')} q^{k(\mathcal{G}')}, \quad p, q > 0, \quad (2)$$

known as the random-cluster (RC) model [26]. Here, $b(\mathcal{G}')$ denotes the number of active edges out of a total number \mathcal{E} of edges of \mathcal{G} , and $k(\mathcal{G}')$ is the resulting number of connected components in the spanning subgraph $\mathcal{G}' \subseteq \mathcal{G}$. Variation of q allows the model to describe a wide range of fractal structures and different connectivities [27], thus accounting for the differences in mechanical response of a range of materials [28,29]. The model includes as particular limits percolation ($q \rightarrow 1$) and the Ising model ($q = 2$). As p is increased, a giant or percolating cluster appears in the system. For sufficiently large q , this transition is of first

order, while for small q it is continuous. For the square lattice the transition occurs at coupling $p_c = \sqrt{q}/(q + \sqrt{q})$, being continuous for $q \leq 4$ [30].

The fragmentation processes discussed here start from an equilibrium configuration of the RC model (2) with bond weight p . The removal of a randomly chosen bond can result in a breakup, creating an additional fragment. In this case, the bond is called a *bridge*. Such a consumption of bridges can serve as a model for the degradation of porous material such as in the combustion of charcoal particles [31]. Similarly, it may describe the breaking of chemical bonds in polymers. The structural resilience under bond removal then depends on the density \mathcal{B} of bridges among all active bonds \mathcal{N} . Figure 1 shows $\langle \mathcal{B}/\mathcal{N} \rangle$ for the equilibrium square-lattice RC model. Incidentally, it is seen that the change of the relative bridge density and hence the change in fragility of the configuration becomes maximal at the critical coupling p_c . This is when a significant fraction of fragmentation events first appears, an effect connected to the (self-)entanglement of critical clusters [32]. In particular, as will be shown below, the behavior of $\langle \mathcal{B}/\mathcal{N} \rangle$ near p_c is governed by the specific-heat exponent α , which implies a divergent slope for $q \geq 2$.

Let us first discuss what happens for a single bond removal if we start at the critical point $p = p_c$ at time $t = 0$. What is the form of $a(s)b(s, s') \equiv a(s, 0)b(s, s', 0)$ for this case? A standard ansatz for Eq. (1) is $a(s) \sim s^\lambda$, where a range $\lambda \leq 1$ of values is found in experiments [1]. A *shattering transition* occurs for $\lambda \rightarrow 0$ [34,35]. To determine λ for the critical RC model, consider the total number of bridges

$$\frac{\sum_s s n(s, 0) a(s)}{\sum_s s n(s, 0)} \sim \int s^{-\tau+1+\lambda} e^{-cs} ds \sim L^{(\tau-\lambda)/(\sigma\nu)}, \quad (3)$$

where we have used the scaling form of the critical FSD $n(s, 0) \sim s^{-\tau} e^{-cs}$ as well as the relations $c \sim |p - p_c|^{1/\sigma}$

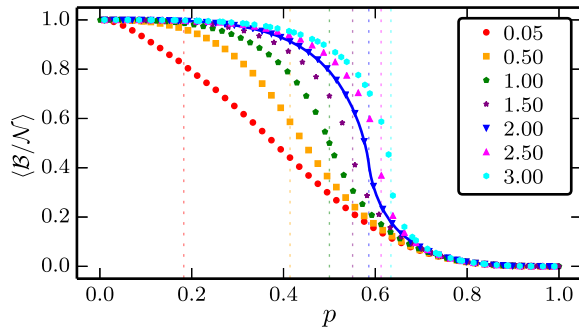


FIG. 1 (color online). Mean proportion of bridges among active edges in the equilibrium random-cluster model for different values of q . Simulation data are for system sizes $L = 64$ ($q \neq 1$) and $L = 2048$ ($q = 1$), respectively. The solid line denotes the exact result for $q = 2$ and $L \rightarrow \infty$. The vertical dashed lines specify the location of the critical point. Simulations were performed using the algorithm described in Ref. [33].

and $|p - p_c| \sim L^{-1/\nu}$, where L is the linear dimension, and ν, σ, τ are standard critical exponents [28]. From Fig. 1 it appears that the density of bridges is asymptotically nonvanishing. This is seen more clearly in our results for the critical bridge density shown in Fig. 2(a). Hence, the average number of bridges in Eq. (3) must grow as L^d , implying $d = (\tau - \lambda)/\sigma\nu$. With the exponent identities $\sigma\nu = 1/d_F$ and $\tau = 1 + d/d_F$, where d_F is the critical cluster fractal dimension, this shows that

$$\lambda = 1, \quad (4)$$

independent of q . Hence, the breakup is spatially homogeneous. This confirms previous numerical results for $q \rightarrow 1$ [24,36].

While Eq. (4) rests on the numerical observation of Fig. 2 for the square lattice, it is more general. By applying a rigorous analysis of the *influence* of an edge [26], we can express the p derivative of the corresponding partition function Z_{RC} in terms of $\langle \mathcal{B} \rangle$ and equate this expression with the standard result, identifying the p derivative of Z_{RC} with $\langle \mathcal{N} \rangle$ [32]. We deduce that for the RC model on an arbitrary graph the bridge and bond densities $\langle \mathcal{B} \rangle$ and $\langle \mathcal{N} \rangle$ are related as

$$\langle \mathcal{B} \rangle = \frac{\langle \mathcal{N} \rangle - p}{(1-p)(1-q)} \quad (5)$$

such that, in general, the bridge density is nonvanishing whenever the edge density is positive. The singular case

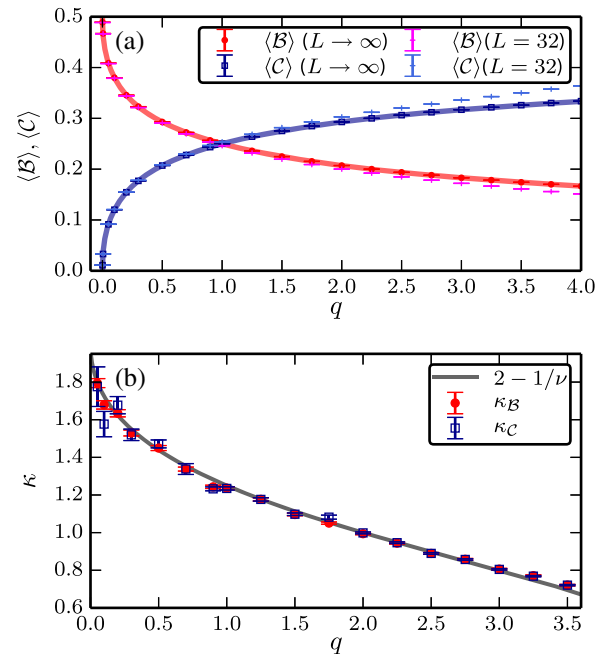


FIG. 2 (color online). (a) Asymptotic critical density of bridges, $\langle \mathcal{B} \rangle$, and nonbridges, $\langle \mathcal{C} \rangle$. (b) Finite-size correction exponent κ for the bridge density according to Eq. (7) for the random-cluster model on the square lattice.

$\langle \mathcal{N} \rangle = p$ corresponds to the percolation limit $q \rightarrow 1$, for which a closer analysis shows that $\langle \mathcal{B} \rangle$ still is finite. Hence, Eq. (4) holds for the RC model on any graph for any bond probability $0 < p < 1$, on or off criticality. For the square lattice, the critical edge density is $\langle \mathcal{N} \rangle_c = 1/2$ [30], such that we find the exact expression

$$\langle \mathcal{B} \rangle_c = \frac{1}{2} \frac{1}{1 + \sqrt{q}}, \quad (6)$$

generalizing a recent result for percolation [37]. Figure 2(a) shows our simulation data together with the asymptotic result (6). Relation (5) shows that the finite-size corrections to $\langle \mathcal{B} \rangle$ are given by the corrections to the edge density $\langle \mathcal{N} \rangle$, which in turn is related to the energy density of the Potts model $u = -2\langle \mathcal{N} \rangle/p$ [26]. Standard scaling arguments [38] lead to

$$u_L = u_\infty + A_u L^{-\kappa} + o(L^{-\kappa}), \quad (7)$$

where $\kappa = (1 - \alpha)/\nu = d - 1/\nu$, in agreement with our data for the finite-size corrections to the density of bridges shown in Fig. 2(b). As a consequence of Eq. (5) one can show that the p derivative of $\langle \mathcal{B} \rangle(p)$ has a power-law singularity at the critical point p_c . This is governed by the specific-heat exponent α . Similar results can be derived for the density $\langle \mathcal{C} \rangle$ of nonbridges [32].

Cluster breakup rates are hence proportional to the cluster size. The typical size of fragments created in a breakup at criticality is encoded in the probability $b(s, s')$. The scale-free nature of the critical RC model suggests a large- s scaling form

$$b_{s',s} \sim s^{-\phi} \mathcal{G}\left(\frac{s'}{s}, \frac{s}{L^{d_F}}\right), \quad (8)$$

which is compatible with exact results for percolation in 1D and on the Bethe lattice [22]. To relate ϕ to previously established critical exponents, we multiply Eq. (8) by s' and then integrate to find that $\mu_s \sim s^{2-\phi} \mathcal{H}(s/L^{d_F})$. Using a finite-size scaling form of the overall FSD [27] we conclude that the scaling of the ensemble average daughter cluster size is $\langle s' \rangle \sim L^{d_F(3-d/d_F-\phi)}$. On the other hand, one can show [32] that this is proportional to the average of $C_{\min,2}$, the size of the smaller of the two clusters attached to two neighboring disconnected vertices [27,33]. In Ref. [27] it was shown that $\langle C_{\min,2} \rangle \sim L^{d_F-x_2}$, where x_2 is known as the two-arm exponent, which implies

$$\phi = 2 + (x_2 - d)/d_F = 2 - d_R/d_F, \quad (9)$$

where $d_R = d - x_2$ is the red-bond fractal dimension, and d denotes the spatial dimension. Again, this confirms and generalizes previous results for bond percolation [23,36]. Another special case concerns the uniform spanning tree

ensemble $p, q \rightarrow 0$ with $q/p \rightarrow 0$ for which $\phi \rightarrow \frac{11}{8}$, in agreement with Ref. [17]. As the data in Fig. 3(b) show, our numerical simulations for the full range $0 \leq q \leq 4$ are in perfect agreement with Eq. (9). More generally, Fig. 3(a) demonstrates the validity of the scaling form of Eq. (8), showing an excellent collapse of data for different cluster and system sizes onto scaling functions parametrized by q . Notably, in contrast to recent claims in Ref. [39], for the RC model clusters do not typically break up into equally sized fragments.

We now generalize to the case of dynamic or continuous fragmentation processes, corresponding to the sequential removal of bonds, or $t > 0$. In general, we must then expect the equilibrium description to break down and $c(s, s', t)$ to be time dependent. Random bond removal drives any initial configuration into an absorbing state where all fragments only consist of one vertex. For real fragmentation processes, however, one rather expects a critical particle size s_c , below which there is no further breakup [1]. This could come about, for instance, through surface tension for the breakup of droplets, via the chosen geometry in a mill, or through energetic limitations in nuclear fragmentation events. Limited fragmentation has been studied for simpler geometries such as intervals and trees [18–20,40] (see also Ref. [31]). For fragmentation processes again starting from critical equilibrium configurations (here for $q \rightarrow 1$), the final FSD below the cutoff s_c is shown in Fig. 4(a). Over a range of fragment sizes increasing with s_c , the data clearly

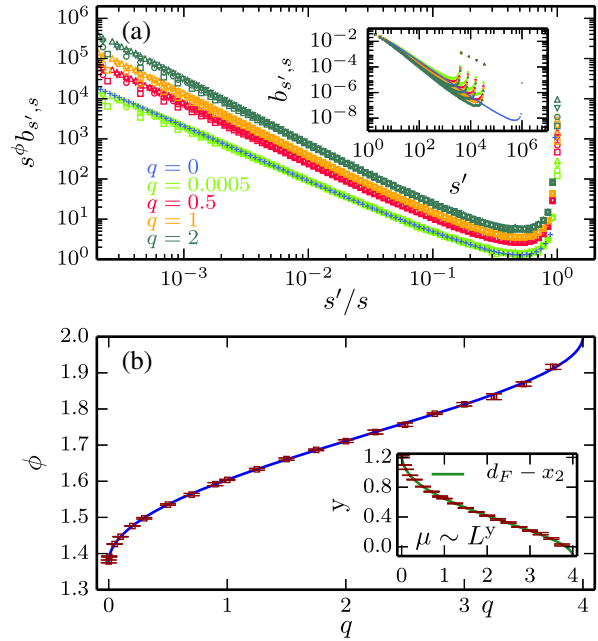


FIG. 3 (color online). (a) Rescaled conditional fragmentation probability $b(s', s)$ according to Eq. (8) for different values of the cluster coupling q . (b) Scaling exponent ϕ of daughter clusters in the fragmentation of the square-lattice RC model as compared to the exact result (9). The inset shows the scaling exponent of the ensemble average daughter cluster size $\langle s' \rangle$.

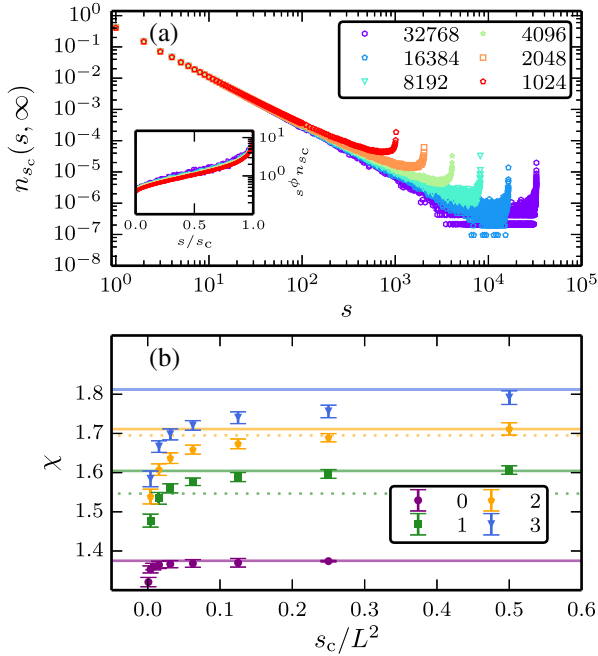


FIG. 4 (color online). (a) Final FSD from iterative fragmentation of the critical giant component for $q \rightarrow 1$ and different values of the cutoff s_c ($L = 256$). (b) Dynamical fragmentation exponent χ according to Eq. (10) for critical initial configurations of cluster weight q . The solid horizontal lines mark the exact values of ϕ in 2D and the dotted lines show estimates of ϕ for 3D [41].

follow a power law. Additionally, the dependence on s_c is only via the ratio s/s_c , resulting in a scaling form

$$n_{s_c}(s, \infty) \sim s^{-\chi} \mathcal{F}\left(\frac{s}{s_c}\right) \quad (10)$$

with a dynamic fragmentation exponent χ . Figure 4(b) summarizes the result of power-law fits to the decay displayed in Fig. 4(a) for different cluster weights q . For sufficiently large cutoffs, we find that χ coincides with the exponent $\phi = 2 - d_R/d_F$ characteristic of equilibrium fragmentation. The deviations for $s_c/L^2 \ll 1$ are an effect of the scaling function \mathcal{F} of Eq. (10). Moreover, not only the power-law decay but the full scaling form (10) of the final FSD is fully supported by our data, as is illustrated in the scaling collapse shown in the inset of Fig. 4(a).

While the close relation of dynamical fragmentation with critical equilibrium properties is at first surprising, it can be understood from the nature of the breakup process. Due to the shape of the breakup kernel shown in Fig. 3, the process is dominated by “abrasive” breakup, i.e., small daughter clusters. Representing the fragmentation events in a genealogical tree, we indeed typically find one long branch, related to the erosion of the giant component, with subbranches of only a few steps [32]. In contrast, uniform breakups would result in a statistically balanced genealogical tree [20]. We hence find the basic assumption in the mean-field model (1) of taking the breakup kernel $c(s, s')$

to be independent of time to be rather appropriate for the model studied here.

In summary, we have first given a scaling description of the fragmentation of critical configurations in the RC model. The density of fragmenting edges is independent of cluster size, implying $\lambda = 1$. The daughter-size function assumes a scaling form with a scaling index connected to the two-arm exponent. Further conclusions follow from the general result (5) [32]. Investigating the asymptotic FSD under continuous fragmentation with a cutoff s_c , we find that this nonequilibrium process is determined by the equilibrium critical behavior with a final FSD described by the equilibrium exponent ϕ . The FSD hence reveals structural characteristics of the initially fragmented object. The insensitivity to microscopic details implied by the universality of critical phenomena indicates that our results for dynamic fragmentation should be comparable also to experiments. In fact, the size exponents found experimentally span a range of around 1.2 to 1.9 [1,8,42], which is also covered by our model on varying q , cf. Fig. 4.

We have restricted ourselves to the case of bond fragmentation. A more general situation occurs for the deletion of vertices producing up to z fragments, where z is the coordination number of the lattice. In this case we find that the binary branch is still strongly dominant. Preliminary investigations indicate a connection between the statistics of such breakup events and generalizations of Eq. (8), where the scaling exponents $\phi^{(k)} = 2 - (d - x_k)/d_F$ of breakups with k fragments are governed by the corresponding multiarm exponents x_k [27].

Our results also carry over to lattices in 3D. In fact, we have studied the fragmentation of clusters of Eq. (2) on the simple cubic lattice and confirmed that $\lambda = 1$. Selected results for the value of ϕ in 3D also shown in Fig. 4(b) indicate that a very similar range of FSDs can be described there. For the dynamical fragmentation process, we find that fragmenting solid instead of fractal objects also leads to algebraically decaying FSDs, however governed by a different set of exponents [32]. Beyond the implications of the present work for fragmentation processes in nature and industry, an exciting extension concerns the fragmentation of random graphs and networks in order to model resilience.

We thank Timothy M. Garoni and Youjin Deng for valuable discussions. We acknowledge funding from the Deutsche Forschungsgemeinschaft (WE4425/1-1) and the 7th Framework Programme of the European Commission (PIRSES-GA-2013-612707).

*ren.metin.elci@gmail.com

†martin.weigel@coventry.ac.uk

‡nikolaos.fytas@coventry.ac.uk

[1] S. Redner, in *Statistical Models for the Fracture of Disordered Media*, edited by H. J. Herrmann and S. Roux (Elsevier, Amsterdam, 1990), pp. 321–348.

- [2] R. M. Ziff and E. D. McGrady, *Macromolecules* **19**, 2513 (1986).
- [3] K. R. Housen and K. A. Holsapple, *Icarus* **84**, 226 (1990).
- [4] A. P. Siebesma, R. R. Tremblay, A. Erzan, and L. Pietronero, *Physica (Amsterdam)* **156A**, 613 (1989).
- [5] M. Kleine Berkenbusch, W. Bauer, K. Dillman, S. Pratt, L. Beaulieu, K. Kwiatkowski, T. Lefort, Hsi, V. E. Viola, S. J. Yennello *et al.*, *Phys. Rev. Lett.* **88**, 022701 (2001).
- [6] D. S. Callaway, M. E. J. Newman, S. H. Strogatz, and D. J. Watts, *Phys. Rev. Lett.* **85**, 5468 (2000).
- [7] M. Newman, *Networks: An Introduction* (Oxford University Press, Oxford, 2010).
- [8] J. A. Åström, *Adv. Phys.* **55**, 247 (2006).
- [9] Z. Danku and F. Kun, *Phys. Rev. Lett.* **111**, 084302 (2013).
- [10] H. A. Carmona, F. K. Wittel, and F. Kun, *Eur. Phys. J. Spec. Top.* **223**, 2369 (2014).
- [11] L. Oddershede, P. Dimon, and J. Bohr, *Phys. Rev. Lett.* **71**, 3107 (1993).
- [12] T. Kadono, *Phys. Rev. Lett.* **78**, 1444 (1997).
- [13] J. A. Åström, R. P. Linna, J. Timonen, P. F. Møller, and L. Oddershede, *Phys. Rev. E* **70**, 026104 (2004).
- [14] F. Wittel, F. Kun, H. J. Herrmann, and B. H. Kröplin, *Phys. Rev. Lett.* **93**, 035504 (2004).
- [15] Z. Cheng and S. Redner, *Phys. Rev. Lett.* **60**, 2450 (1988).
- [16] P. L. Krapivsky and E. Ben-Naim, *Phys. Rev. E* **50**, 3502 (1994).
- [17] S. S. Manna, D. Dhar, and S. N. Majumdar, *Phys. Rev. A* **46**, R4471 (1992).
- [18] P. L. Krapivsky, I. Grosse, and E. Ben-Naim, *Phys. Rev. E* **61**, R993 (2000).
- [19] P. L. Krapivsky and S. N. Majumdar, *Phys. Rev. Lett.* **85**, 5492 (2000).
- [20] D. S. Dean and S. N. Majumdar, *J. Phys. A* **35**, L501 (2002).
- [21] Z. Kalay and E. Ben-Naim, *J. Phys. A* **48**, 045001 (2015).
- [22] M. F. Gyure and B. F. Edwards, *Phys. Rev. Lett.* **68**, 2692 (1992).
- [23] J.-M. Debierre, *Phys. Rev. Lett.* **78**, 3145 (1997).
- [24] M. Cheon, M. Heo, I. Chang, and D. Stauffer, *Phys. Rev. E* **59**, R4733 (1999).
- [25] S. B. Lee, *Physica (Amsterdam)* **393A**, 480 (2014).
- [26] G. Grimmett, *The Random-Cluster Model* (Springer, Berlin, 2006).
- [27] Y. Deng, W. Zhang, T. M. Garoni, A. D. Sokal, and A. Sportiello, *Phys. Rev. E* **81**, 020102 (2010).
- [28] D. Stauffer and A. Aharony, *Introduction to Percolation Theory*, 2nd. ed. (Taylor & Francis, London, 1994).
- [29] C. P. Broedersz, X. Mao, T. C. Lubensky, and F. C. MacKintosh, *Nat. Phys.* **7**, 983 (2011).
- [30] F. Y. Wu, *Rev. Mod. Phys.* **54**, 235 (1982).
- [31] J. Huang, X. Guo, B. F. Edwards, and A. D. Levine, *J. Phys. A* **29**, 7377 (1996).
- [32] E. M. Elçi, M. Weigel, and N. G. Fytas (to be published).
- [33] E. M. Elçi and M. Weigel, *Phys. Rev. E* **88**, 033303 (2013).
- [34] N. F. Mott, *Proc. R. Soc. A* **189**, 300 (1947).
- [35] E. D. McGrady and R. M. Ziff, *Phys. Rev. Lett.* **58**, 892 (1987).
- [36] B. F. Edwards, M. F. Gyure, and M. Ferer, *Phys. Rev. A* **46**, 6252 (1992).
- [37] X. Xu, J. Wang, Z. Zhou, T. M. Garoni, and Y. Deng, *Phys. Rev. E* **89**, 012120 (2014).
- [38] V. Privman, in *Finite Size Scaling and Numerical Simulation of Statistical Systems*, edited by V. Privman (World Scientific, Singapore, 1990), pp. 1–98.
- [39] M. Schröder, S. E. Rahbari, and J. Nagler, *Nat. Commun.* **4**, 2222 (2013).
- [40] S. N. Majumdar and P. L. Krapivsky, *Phys. Rev. E* **65**, 036127 (2002).
- [41] Y. Deng, T. M. Garoni, and A. D. Sokal, *Phys. Rev. Lett.* **98**, 230602 (2007).
- [42] G. Timár, J. Blömer, F. Kun, and H. J. Herrmann, *Phys. Rev. Lett.* **104**, 095502 (2010).